sustainability

MDPI

Article

A Study on the Train-Induced Vibration Responses of Heavy Haul Railway Subgrade in Seasonally Frozen Regions Using Field Experiments

Yu-Zhi Zhang [1,2,*], Ya-Qian Dong [3], Xiu-Xiu Cao [3] and Pei Li [4]

[1] Key Laboratory for Health Monitoring and Control of Large Structures in Hebei Province, Shijiazhuang Tiedao University, Shijiazhuang 050043, China
[2] Collaborative Innovation Center for Performance and Safety of Large-Scale Infrastructure, Shijiazhuang Tiedao University, Shijiazhuang 050043, China
[3] School of Civil Engineering, Shijiazhuang Tiedao University, Shijiazhuang 050043, China
[4] Geotechnical and Underground Engineering Research Institute, Beijing University of Technology, Beijing 100124, China
* Correspondence: zhangyuzhi@stdu.edu.cn; Tel.: +86-159-3019-3076

Abstract: The dynamic response resulting from heavy haul train leads to the deterioration of the railway subgrade, especially those built in seasonally frozen regions. In this work, a typical heavy haul railway section in a seasonally frozen region is monitored on-site. The time domain and the frequency domain analysis of the subgrade vertical vibration acceleration, dynamic speed, and displacement during the non-frozen period and the frozen period are investigated. The results show that the vibration response of the subgrade is affected by various factors, including the train type, locomotive, traveling speed, train formation, heavy load, and the prevalent season. Further, it is observed that the maximum and average vertical acceleration of the subgrade, the vibration speed, and the dynamic displacement increase during the frozen period. However, the main frequency of the natural vibration remains significantly higher than that before freezing. Moreover, the frozen soil has a significant amplification effect both on the acceleration and the attenuation rate. Similarly, the subgrade's vibration mode has a low frequency and high amplitude during the freezing period, and the dynamic response characteristics become increasingly apparent as the axle load increases.

Keywords: seasonally frozen region; heavy haul railway subgrade; dynamic response; vibration acceleration; on-site monitoring

Citation: Zhang, Y.-Z.; Dong, Y.-Q.; Cao, X.-X.; Li, P. A Study on the Train-Induced Vibration Responses of Heavy Haul Railway Subgrade in Seasonally Frozen Regions Using Field Experiments. *Sustainability* **2022**, *14*, 15954. https://doi.org/10.3390/su142315954

Academic Editors: Weiguang Zhang, Ruxin Jing, Feng Zhang, Rui Zhang and Chuang Lin

Received: 13 October 2022
Accepted: 25 November 2022
Published: 30 November 2022

1. Introduction

The heavy haul railway, which has seen rapid development over the years, is the symbol of national railway freight modernization. Countries such as China and USA are actively promoting the operation of heavy-haul trains. China has been developing heavy-haul transportation since the 1980s, establishing its position as the industry leader in heavy-haul railways. China has completed 25% of the world's railway workload with 6% of the world's railway mileage. Being the world's third largest country in the frozen soil region, China has several heavy haul railways that encompass frozen regions. These include the Datong–Qinhuangdao Railway, the Shuozhou–Huanghua port (ShuoHuang) Railway, and the Jungar–Shenmu Railway. The main foundation of the track structure of the heavy haul railway in China is subgrade (typically above 70%). Previous studies on heavy haul railway diseases show that the dynamic load amplitude of heavy haul railway subgrade increases when the axle load and operation speed increase during the operation of long and large group trains. However, the dynamic strength decreases under these conditions. The line subgrade in frozen soil regions frequently suffers from haul railway disease [1,2], thus posing a serious threat to train safety and driving up maintenance and

operation expenses. As the service life is extended and the operation of the trains continues in long marshaling and large axle load, the constructed heavy haul railway subgrade gradually exhibits more severe issues in dynamic stability and service life under repeated freeze–thaw cycles. This, in turn, severely restricts the development of heavy-haul railways in frozen regions of China. The larger the carrying capacity of the train, the stronger the interaction between the train and the railway track structure, thereby leading to more serious dynamic damage and unevenness of the railway subgrade and track structure [3]. Not only does it have an impact on the safety and stability of train operation on elastic track structures, but it also reduces the reliability of the pantograph–catenary system [4]. The dynamic response of the subgrade reflects the interaction between the train and the subgrade. In order to ensure the safety, smoothness, and efficient operation of trains, it is necessary to comprehensively demonstrate the subgrade dynamic response law and systematically understand the changes in subgrade performance, which in turn provides a theoretical basis for weakening the dynamic interaction between heavy haul trains and tracks.

Various approaches, including indoor/outdoor model tests, theoretical models, on-site monitoring, and the combined multiple methods, are currently adopted for studying the characteristics of train-induced vibration responses of subgrade [5]. The indoor large-scale model experiment method [6] is employed for analyzing the impact of climate, soil conditions, and engineering measures on the dynamic response of subgrade. Gao et al. [7] and Omer et al. [8] suggested that the Finite element numerical method can help in investigating the impact of the water content, train speed, and environmental temperature of subgrade on the safety, comfort, and stability of the railway. Li et al. [9] reported that the dynamic response of the permafrost subgrade could be evaluated using the exciting force function composed of static load and a series of sine functions as the train load. They further suggest that, when the temperature is taken into account, the soil may be considered as a simplified Mohr–Coulomb model. Bahrekazemi et al. [10] and Ren et al. [11] reported the development of empirical models based on field data and soil dynamic parameters for estimating the vibration response of soil at different depths. The analytical method and empirical prediction models, however, require several restrictions and simplifications concerning the geometry and material properties of the problem. Therefore, it is very challenging to find a closed solution or to conduct a thorough analysis of the influencing factors to address the issue of train vibration under these complex conditions. On-site monitoring does not only provide the theoretical and experimental models (e.g., finite element numerical model) with valuable supplementary data for comparison and verification [12,13] but also is an effective method for studying train-induced vibration response of subgrade. Petriaev [14] carried out a fielding monitoring experiment to study the foundation bed's dynamic response to heavy haul trains. The results showed a significant reduction in the dynamic response of the foundation bed upon the increase in the train load and speed. Vibration acceleration of subgrade is the main index for assessing the damaging effect of vibration on track structure [15]. The results of the research study show that the acceleration response of ballasted track of the high-speed railway is associated with the train speed and the distance from the track center. It has also been observed that it increases as the train speed increases and decreases as the distance from the track center decreases [16]. Researchers are now focusing on the vibration responses of the subgrade in the frozen regions due to the ongoing construction and operation of railways in cold regions. Zhu et al. [17] compared the vibration response characteristics and attenuation laws of vibration that were transmitted in steel rail, sleeper, and subgrade running at a normal speed for a thermal probe subgrade and a general subgrade of Qinghai–Tibet Railway in the permafrost area as well as the subgrade in seasonally frozen regions. Chen et al. [18] conducted real-time strong vibration tests on the right shoulder, left, and right slope feet of the typical subgrade of Qinghai–Tibet Railway in the Beiluhe in the warm season. They obtained the vibration acceleration attenuation laws of the railway subgrade in the permafrost region. The results of the field acceleration tests [19,20] for the Harbin–Dalian

Railway's common passenger and freight lines in seasonally frozen regions showed that the dynamic response increased as train speed, the number of cars, and load increased. Further, the vertical and longitudinal accelerations exhibit an increase during the freezing period but a decrease during the melting period. A review of the previous literature shows few reports of on-site vibration monitoring of heavy haul railway subgrades, particularly those in frozen regions. Dong et al. [21] monitored the vertical accelerations of different heavy haul trains from the embankment shoulder surface to the area 70 m beyond the toe of the Datong–Qinhuangdao heavy haul railway. The vibration accelerations during winter were found to be 13–26% higher than those during the non-frozen period. The above study improves our understanding of how the subgrade's vibration responses varied depending on the direction and distance from the track and the type of train. However, the shortcoming was that the ground temperature change data were not measured at the same time, and therefore the freezing depth during the freezing period was not obtained. Moreover, the acceleration sensors were usually at a distance from the track structure due to normal operation. The closest monitoring sites were usually placed in the shoulder position, which lay at a distance of more than 2 m from the outer rail of the line. Therefore, the vibration response at the most relevant location under the trains could not be directly measured. Moreover, the monitoring sites were usually only deployed on one line of the dual-line subgrade. In the case of heavy haul railways with distinct full- and no-load lines, the investigation of vibration responses of the subgrades beneath the train with different axle loads and two lines, particularly the vibration responses of individual subgrades beneath the rail, would contribute to the systematic understanding of the change in the subgrade performance.

In this work, a typical section of heavy haul railway subgrade and laid ground temperature and acceleration monitoring sites at various depths of the subgrade are selected based on observations from the literature. The acceleration test is performed on the subgrade surface beneath the rail. This paper has the following structure: Initially, the on-site monitoring section and site arrangement are introduced. Then, the impact of train type, traveling speed, and operation status (full-load or no-load) on the vibration response of double-track subgrade surface during the non-frozen period are investigated. The vibration responses of subgrade during the non-frozen period and the freezing period are compared. Thereafter, the frequency-domain and time-domain analyses on vibration responses of the subgrade are performed. Finally, the vibration response characteristics, such as speed and dynamic displacement caused due to the subgrade vibration, are analyzed. This work helps to fully demonstrate the subgrade dynamic response law, and the results can provide a theoretical base for the detection of subgrade frost heave disease in cold regions and offer monitoring data support for related theoretical calculation models.

2. Monitoring Sites and Site Arrangements

2.1. Monitoring Sites

The ShuoHuang Railway is the largest double-track electrified joint venture railway in China. It is also the second largest route for transporting coal from west to east in China. It accelerates local economic development along the route and guarantees energy supply to east and southeast coastal areas. Further, it is of great strategic significance in terms of China's coal export capacity expansion. The ShuoHuang Railway is located in the hilly area from West Ningwu to South Shenchi. Generally, winter begins in October every year and ends in April the next year. Uneven frost heave deformation along the subgrade and uneven heave compression deformation in the spring thaw period leads to frequent freezing damage. Although plenty of time and effort is put into detection, maintenance, and rehabilitation, the results are still not satisfactory. Thus, it restricts the normal operation of the railway. Therefore, in this work, the ShuoHuang Railway in Shenchi County, Xinzhou city, Shanxi Province, was selected for on-site monitoring for the dual-line section. This site is located in a typical seasonally frozen region. The subgrade surface width is 11.1 m, and the no-load line is a cutting. Further, the full-load line is

an embankment, the national railway line is under the slope, and the shoulder width is 1.5 m. The average temperature of the coldest month is −7.7 °C, and the maximum freezing depth is 1.1 m. The area is vulnerable to significant frost damage, according to inspection data collected throughout the operation time, and is also thought to have a high prevalence of several diseases. Figure 1 shows the geographical locations of ShuoHuang Railway and the monitored section.

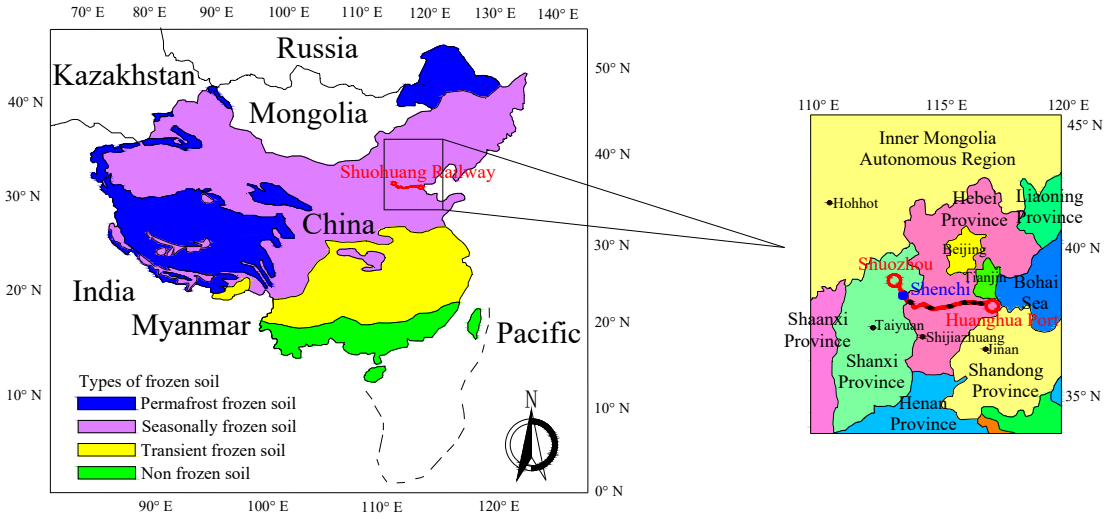

(**a**)

(**b**)

Figure 1. (**a**) Geographical locations of the ShuoHuang Railway and (**b**) the monitored section.

2.2. Site Arrangements

The test section in the site arrangement is a dual line. Full-load trains bound for the Huanghua Port through C1 and no-load trains back to Shuozhou through C2 are monitored. Ground temperatures at various depths and positions of the subgrade, as well as the acceleration of the subgrade surface soil beneath the track, are among the monitored indices of ground temperature and dynamics characteristics of the heavy haul railway subgrade in the seasonally frozen regions.

Figure 2 shows the monitoring sites on the subgrade. The monitoring sites for ground temperature are placed at 0.2, 1.0, 2.0, 3.0, and 4.0 m below the no-load line shoulder, as well as 0.2, 0.5, 1.0, and 2.5 m below the line center and full-load line subgrade. Therefore, there are 13 monitoring sites in total, with two monitoring sites observed for vibration acceleration of the subgrade. They are arranged 0.2 m below the top surface of the subgrade, where C1 is right below the track rail of the full-load line, and C2 is right below the track rail of the no-load line. The distance between the two lines is 4.0 m, and the distance between the two acceleration sensors is about 5.5 m.

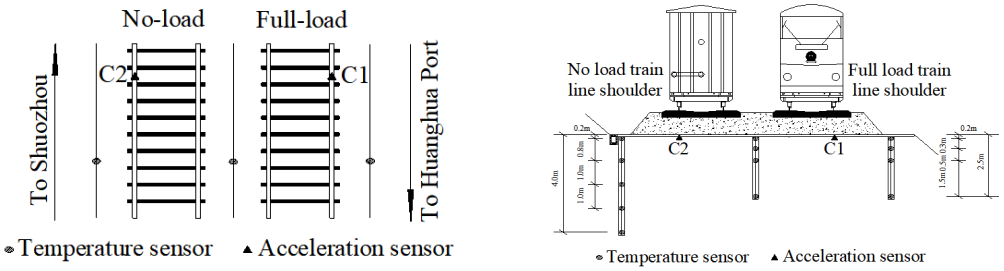

(**a**) (**b**)

Figure 2. Sensor arrangement: (**a**) longitudinal sensor arrangement; (**b**) transverse sensor arrangement.

By analyzing the local climate, freezing depth, filling and digging forms of subgrade, groundwater level depth, and subgrade monitoring indicators in Shenchi County, the sensor model, measurement range, and accuracy were determined, as shown in Table 1. The sensors used in this work are shown in Figure 3.

Table 1. List of Sensors used.

Monitoring Index	Sensor Type	Measurement Range	Accuracy
round temperature	PT100 temperature sensor	−40 °C~+60 °C	±0.03 °C within −20 °C~+20 °C
acceleration	MSA1000-02 variable capacitance acceleration sensor	±2 g	0.001 g

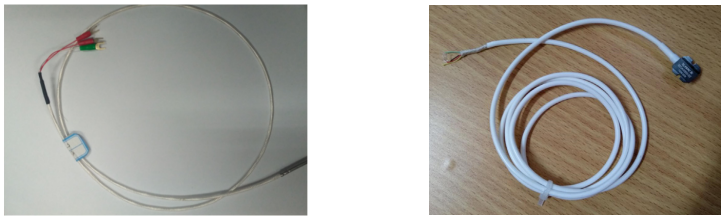

(**a**) (**b**)

Figure 3. Images of (**a**) temperature sensor and (**b**) acceleration sensor.

By considering the equipment protection requirement and field conditions, the shoulder outside the full-load line fence was selected to build the base of the on-site monitoring station. The sensor on the side of the no-load line is led to the collection box of the monitoring base station using a pipe under the ballast. A trench with a length of 15 m, a depth of 0.3 m, and a width of 0.5 m was excavated for the transmission line and was protected using a high-strength PVC pipe. From Figure 4a, the acceleration sensor was embedded at a depth of 0.2 m under the surface of the subgrade, directly beneath the outer rail of the two lines. Further, the sensors were packed in advance. When considering the acceleration sensor's location, the ballast under the steel rail should be removed. The acceleration sensors were therefore installed during the trench excavation.

(**a**) (**b**) (**c**)

Figure 4. Field installation of the monitoring system: (**a**) excavation of a trench to lay a pipe; (**b**) sensor placement; (**c**) sensor calibration.

The filling materials and filling process are required to follow the static matching principle during the embedding process of various sensors. The subgrade soil is mainly composed of yellow silt and reddish-brown clay. The clay is removed layer by layer while digging the holes. The sensors are subsequently installed, and the soil is filled again at the original site.

3. Results

The monitored ground temperature and the characteristics of the vibration response of subgrade induced by different heavy haul trains are discussed below.

3.1. Ground Temperature

The subgrade monitoring system was completed in August 2019, and the commissioning was carried out at the site and the remote end. It was formally put into operation in October 2019, and the system started running normally. The data that were monitored from 17 October 2019 to 14 April 2020 were selected from the temperature monitoring system. Figure 5 shows the time–history curves of the ground temperature at different positions.

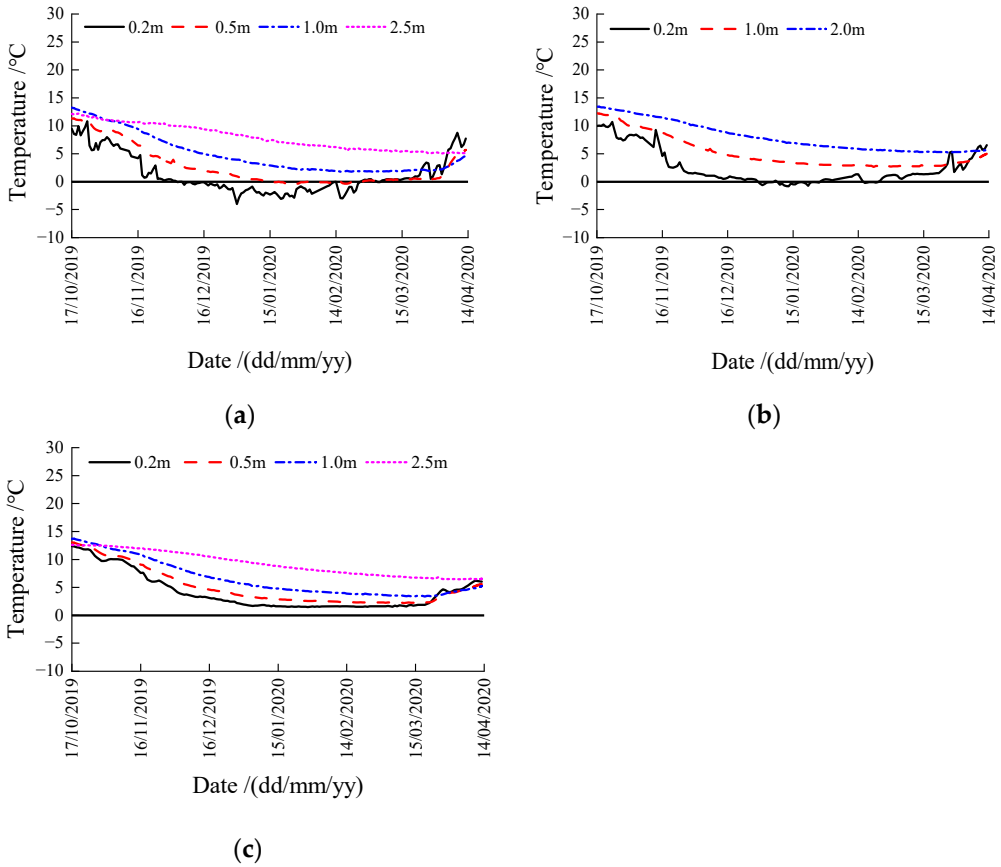

Figure 5. Time–history curves of ground temperature on the monitored section: (**a**) full-load line shoulder; (**b**) no-load line shoulder; (**c**) centerline between two lines.

From Figure 5, it can be observed that the temperature changes near the surface are larger and have certain volatility, which is affected by the atmospheric temperature. The subgrade starts to freeze from the beginning of December 2019, reaching the maximum freezing depth until about mid-January. The lowest temperature of the soil in the subgrade shoulders on both sides is found to be below zero, and the soil is frozen within 0–0.5 m of the subgrade shoulder. Further, the ground temperature amplitude and the freezing depth of the shoulder at the full-load line are observed to be the greatest, while the ground temperature remains the same until mid-February. The atmospheric temperature rises

to positive in spring in late February or early March, and the subgrade melts from top to bottom and completes by mid-March. Furthermore, the lowest temperatures of the subgrade soil between the two lines do not reach negative temperatures and are well above 0 °C.

The starting date of the remote collection using the acceleration monitoring system is 11 November 2019. The acceleration collection frequency interval randomly exceeds 10 days, and 10 sets of data are collected each time. Moreover, different trains are also counted. The vibration acceleration collected in November 2019 is selected as the typical data representing the non-frozen period. The vibration acceleration collected in January 2020 is taken as the typical data of the freezing period.

3.2. Characteristics of Vibration Response of Subgrade Induced by Different Heavy Haul Trains

In order to study the vertical vibrations of the subgrade surface soil in the cases of different trains with different axle loads, data are collected from the trains in the ShuoHuang Railway monitored section K5 + 780 for two consecutive days within a range of 100 m (5.730~5.830 km). The results show that this section of the ShuoHuang Railway's daily operation vehicles includes C64, C70, and C80, grouped as ordinary, 10,000 ton, and 20,000 ton. Table 2 lists the main performance parameters of the three trains. Therefore, the no-load train weight is considered to be the self-weight, and the full-load train weight is considered to be the sum of the self-weight and the carrying capacity. Moreover, the axle load in the table is the average axle load of the total full-load train weight, with the calculation rounded according to four pairs of axles. Therefore, the axle load of full-load and no-load trains are found to follow the orders of C80 > C70 > C64 and C70 > C64 > C80, respectively. Further, the freight cars in the test section are hauled by Shenhua and SS4 locomotives, as shown in Figure 6. Figure 7 shows the monitored vibration acceleration when the Shenhua locomotive crosses the full-load line at low speed. C1 and C2 in Figure 7 represent the two acceleration monitoring points, which are located directly below the full-load line and the no-load line tracks.

Table 2. Main performance parameters of common trains.

Train Type	Formation	Carrying Capacity/t	Self-Weight/t	Axle Load/t	Car Length/m
C64	ordinary	61	≤23	21	134.30
C70	10,000 ton	70	≤23.8	23	139.76
C80	20,000 ton	80	≤20	25	120.00

Figure 6. Heavy haul locomotive of ShuoHuang Railway.

Figure 8 is a schematic diagram of the coach of the C80 heavy haul train traveling on the ShuoHuang Railway. According to the geometric profile of the trains, the heavy haul railway subgrade is subjected to a periodic excitation. Table 3 lists the corresponding fundamental frequency generated according to the geometry and train speed of C80. v in this table means velocity.

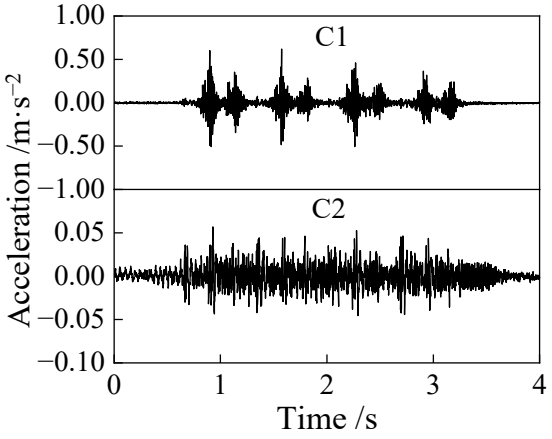

Figure 7. Induced acceleration time–history variation when locomotive passes.

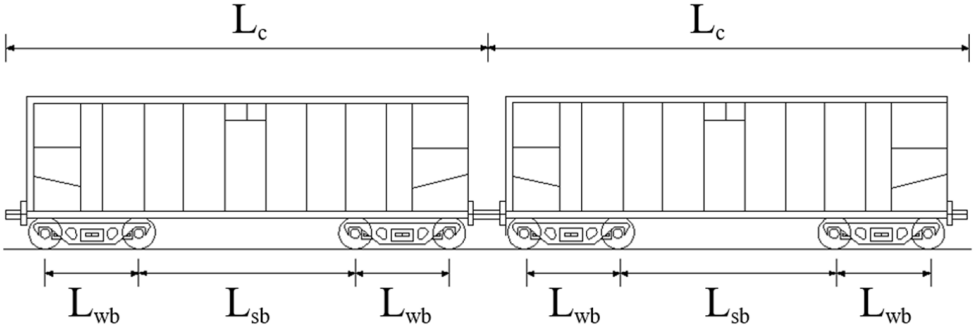

Note: L_c, L_{wb}, and L_{sb} represent the centre distance of two neigh-bouring cars, the wheel base length, the distance between two bogie centres of the same car.

Figure 8. Coach of the C80 train.

Table 3. Characteristic frequencies of heavy haul train (C80) load.

Characteristic Length (m)		Frequencies (Hz)	
		v	55 km/h
L_c	12	f_c	1.27
L_{wb}	1.83	f_{wb}	8.35
L_{sb}	8.2	f_{sb}	1.86

Note: $f_c = v/L_c$, $f_{wb} = v/L_{wb}$, and $f_{sb} = v/L_{sb}$.

From Figure 7, the subgrade in the full-load line experiences a maximum vertical acceleration of 0.50 m/s^2 that is directly caused by the locomotive, while the subgrade experiences a maximum vertical acceleration of 0.05 m/s^2 that is also caused by the locomotive. The acceleration is attenuated by 90%.

The train speed is a major factor influencing maximum and average vibration acceleration. Figure 9 shows the acceleration of the induced subgrade vibration as the train passes at a variable speed. It is evident from Figure 9 that the change in train speed has a significant impact on acceleration, showing a greater uncertainty. In order to reduce the impact of train speed in the analysis of acceleration vibration characteristics, the vibration responses of the subgrade of different trains are selected during different periods with train speeds in the range of 50~60 km/h for analysis.

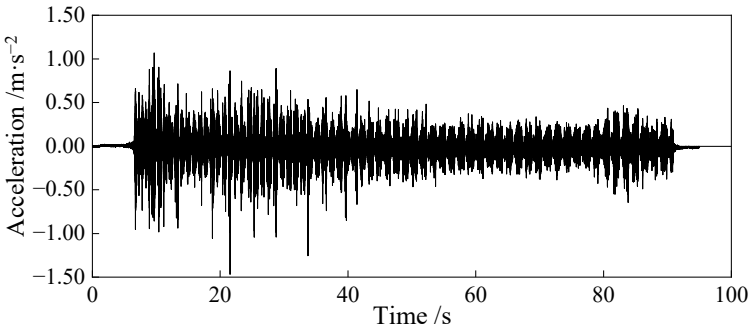

Figure 9. Acceleration time–history variation at C1 when train speed changes.

The vibration response of the railway subgrade is a random composite vibration with complex frequency and amplitude. The on-site acceleration monitoring results reveal the vibration acceleration signal obtained at the site when the train passes each time. Presently, the analysis of monitoring signals is mainly classified into two types, namely, the time domain analysis and the frequency domain analysis. Both types are discussed as follows:

1. Time-domain analysis: Curves that change with time are frequently obtained during the observation of natural or social phenomena, and they are known as time-domain signals. The common time-domain analysis methods include statistical analysis, correlation analysis, and historical trend analysis, with main indexes of maximum, average, and effective values. This study focused on conducting filtration of the acceleration signals collected during the monitoring of the system to obtain the acceleration time–history curve. Thereafter, statistical analysis and correlation analysis were used for the analysis of maximum, average, and effective acceleration.
2. Frequency-domain analysis: Complex signals primarily comprise multiple sinusoidal waves with different frequencies. The composition of the amplitude and phase of the sinusoidal wave is called the spectrum of the signal. The commonly used frequency-domain analysis method is the power spectrum analysis, which includes the self-power spectrum analysis and the cross-power spectrum analysis. These analyses can clearly show the acceleration characteristics of the subgrade. This study also focused on carrying out the Fast Fourier Transform (FFT) of time-domain data of acceleration to obtain the spectrum, i.e., to conduct FFT of acceleration time–history curve to obtain the acceleration spectrum curve.

In order to study the changing laws and attenuation characteristics of the vibration acceleration, this study defines the maximum vertical vibration acceleration, average acceleration, and effective acceleration as the eigenvalue of the vibration response acceleration. This enables the analysis of the vibration intensity caused due to the train load.

After removing the outlier, the maximum vertical vibration acceleration ($|a|_{max}$) refers to the average value of the five maximum absolute values of the recorded accelerations at a different time in one site. It describes the maximum amplitude of the vibration acceleration induced by each heavy haul train and is represented as shown in Equation (1).

$$|a|_{max} = \frac{1}{N}\sum_{i=1}^{N}|a_i|_{max} \ (i = 1, 2, 3 \cdots N) \tag{1}$$

The average vertical vibration acceleration ($|a|_{par}$) refers to the average absolute value of recorded accelerations at a different time in one site. It describes the average vibration acceleration at the sites induced by each heavy haul train and is represented as shown in Equation (2).

$$|a|_{par} = \frac{1}{N}\sum_{i=1}^{N}|a_i| \ (i = 1, 2, 3 \cdots N) \tag{2}$$

The effective vertical vibration acceleration ($|a|_{vol}$) refers to the effective acceleration at a different time in one site. It describes the changing laws and attenuation characteristics of vibration acceleration and is represented as shown in Equation (3).

$$|a|_{vol} = \frac{1}{N}\sqrt{\sum_{i=1}^{N}|a_i|^2}\ (i = 1, 2, 3 \cdots N) \tag{3}$$

In the above equations, a_i refers to the recorded i th vertical acceleration when the train passes; N refers to the number of recorded accelerations when the train passes, which is 10 at most in Equation (1) [22].

In this work, C64, C70, and C80 were selected with a speed of 58 km/h, 54 km/h, and 55 km/h, respectively. It is observed that during the non-frozen period, the three trains pass by C1 in a full-load status, and the directly caused vibration acceleration is measured, while C2 measures the indirectly caused vibration acceleration when the acceleration time–history is varied, as shown in Figure 10.

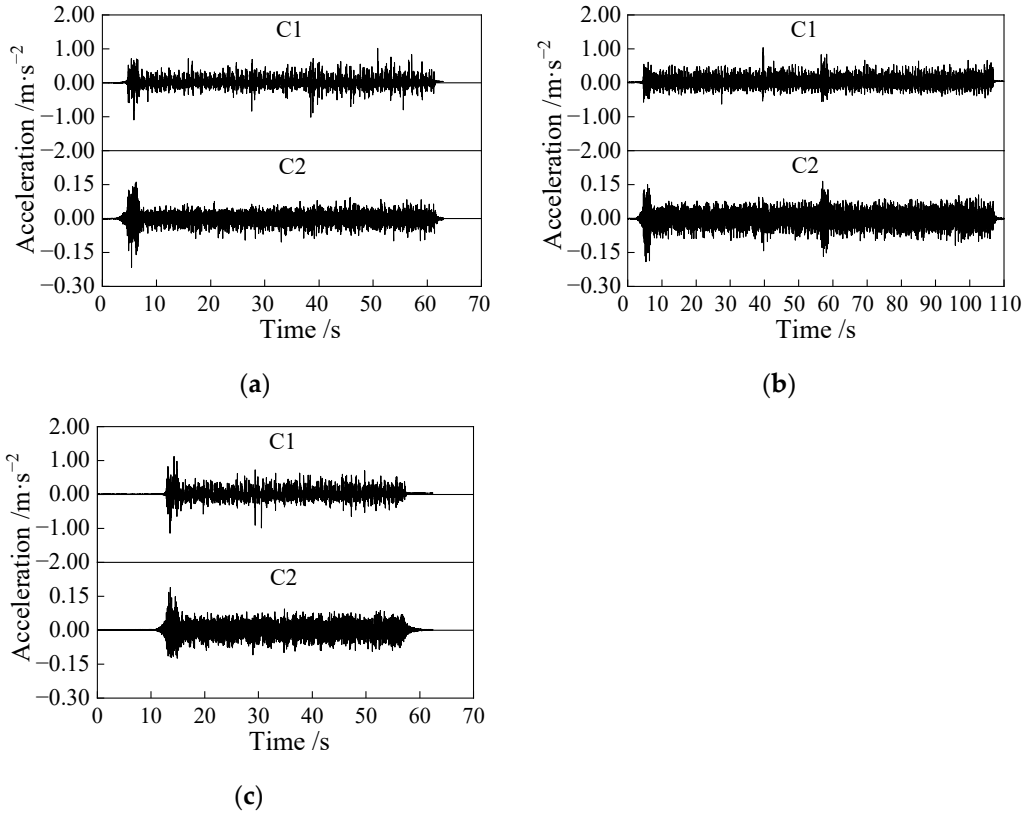

Figure 10. Acceleration time–history curves of full-load train at the sites: (**a**) ordinary C64; (**b**) 10,000 ton C70; (**c**) 20,000 ton C80.

From Figure 10, it can be observed that the subgrade surface vibration acceleration reflects the situations corresponding to different trains and formations, and it has quite evident peaks with periodic changes. Because the speed of the locomotive is greater than that of the coach, a larger value of vertical acceleration is caused by the locomotive. The locomotive-induced vibrations are significant, while coach-induced vibrations are relatively insignificant, and the time for the train to pass by the sites is different due to the difference in train length. Therefore, the maximum locomotive acceleration, average coach acceleration, and train vibration period are used to estimate train type and formation. Further, the induced vibration accelerations of the subgrade measured at C1 and C2 are also increased with the increase in the axle load.

Table 4 lists the train speed and induced maximum ($|a|_{\max}$), average ($|a|_{\mathrm{par}}$), and effective ($|a|_{\mathrm{vol}}$) acceleration of different trains at the sites during the non-frozen period.

The test section is a dual-line section, and the trains left Shenchi Station through C1 in a full-load status. During this duration, it is observed that C1 measures the subgrade vibration acceleration that is directly caused by the full-load trains, while C2 measures the vibration acceleration of the subgrade that is indirectly caused by the trains on the no-load side. On the other side, no-load trains go back to Shenchi Station through C2. Therefore, C2 measures the vibration acceleration of the subgrade that is directly caused by the no-load trains, while C1 measures the vibration acceleration of the subgrade that is indirectly caused by the trains on the full-load side.

Table 4. Vibration accelerations of heavy haul train traveling on the subgrade (m/s^2).

Load	Train Type	Speed/ ($km \cdot h^{-1}$)	C1 (the Full-Load Side)			C2 (the No-Load Side)		
			$\|a\|_{max}$	$\|a\|_{par}$	$\|a\|_{vol}$	$\|a\|_{max}$	$\|a\|_{par}$	$\|a\|_{vol}$
Full-load	C64	56	0.993	0.094	1.794	0.182	0.018	0.318
	C70	55	1.050	0.087	1.198	0.187	0.020	0.267
	C80	52	1.534	0.103	2.536	0.210	0.020	0.219
No-load	C64	50	0.102	0.034	0.321	0.870	0.070	0.824
	C70	58	0.133	0.026	0.302	1.290	0.078	0.951
	C80	60	0.101	0.019	0.269	1.180	0.080	0.656

From Table 4, it is clear that different acceleration eigenvalues generally demonstrate growing trends with the increase in axle load; however, not all of them have the same performance. This can be possibly attributed to the different lengths and speeds of different models themselves. Moreover, it can also be observed that when the full-load heavy haul trains pass by, the maximum and average accelerations of C1 are both larger than those of C2, and the variation is five times larger. Further, the maximum vertical acceleration (1.534 m/s^2) is observed when a full-load C80 (with the maximum axle load) passes by C1. Additionally, it is observed that when no-load trains pass by, the measured acceleration eigenvalues of C2 are significantly greater than those measured at C1 on the full-load line. In this case, the average and eigenvalues of the acceleration measured at C2 are usually 2–4 times larger than those of C1, whereas the maximum acceleration at C2 is 10 times larger than that at C1. Furthermore, when C70 (with maximum axle load) passes, C2 exhibits the maximum vertical acceleration (1.290 m/s^2).

Zhu et al. [23] carried out on-site monitoring of the vibration response on the Harbin–Dalian Railway and collected data on maximum and average absolute acceleration when the train passed. They found that the mean vertical absolute acceleration was 0.108 $m/s^{2,}$ and the maximum vertical vibration acceleration was 1.52 m/s^2 when the freight train passed the monitoring site on the shoulder. The corresponding code for vertical vibration acceleration has a clear assessment limit of 0.18 g [24]. According to Table 4, the comparison with the Harbin–Dalian Railway monitoring data shows that the maximum vibration acceleration of the ShuoHuang heavy haul railway is less than the limit value.

3.3. Vibration Responses of Subgrade before and after Freezing

The results for the time-domain analysis and acceleration eigenvalue, frequency-domain analysis of acceleration, attenuation law of vibration response acceleration of subgrade, and the response features of dynamic speed and dynamic displacement before and after freezing are discussed below.

3.3.1. Time-Domain Analysis and Acceleration Eigenvalue

In order to analyze the vibration characteristics of the subgrade during the freezing period and the non-frozen period accurately, in this study, the collection frequency was increased to 1000 Hz. According to the monitored ground temperature (as shown in Figure 5), the vibration acceleration collected in November 2019 is selected as the typical data for the non-frozen period, whereas the vibration acceleration collected in January

2020 is taken as the typical data for the freezing period. Based on the shoulder ground temperature, it is found that the freezing depth of the shoulder on one side of the full-load line is about 0.36 m. Figure 11 shows the time–history curves of vertical vibration acceleration of subgrades induced by three types of full-load heavy haul trains passing by C1.

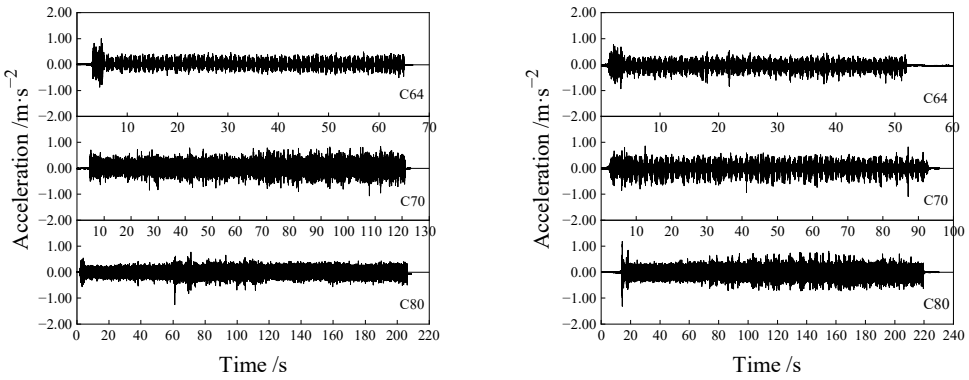

Figure 11. Time–history variation in vibration acceleration induced by full-load trains passing by C1 in different periods: (**a**) non-frozen period; (**b**) freezing period.

As shown in Figure 11, regardless of the frozen or non-frozen period, the vibration acceleration caused by the train increases with the increase in axle weight. Compared with the non-frozen period, the vibration acceleration caused by the same axle weight train during the freezing period is larger. Due to the frozen part of the subgrade, uneven deformation and track unevenness are found to increase. The interaction and vibration between the line and the train increase, and the vibration response of the roadbed consequently increase. The maximum, average, and effective vertical vibration accelerations of subgrade induced by a full-load heavy haul train passing by C1 during the non-frozen period and the freezing period are summarized. Table 5 shows the accelerations passing the monitoring points at similar speeds during the non-frozen period and the freezing period.

Table 5. Vibration acceleration of the ShuoHuang Railway (mm/s^2).

Train Type	Speed/ (km·h^{-1})	During the Non-Frozen Period			Speed/ (km·h^{-1})	During the Freezing Period		
		$\|a\|_{max}$	$\|a\|_{par}$	$\|a\|_{vol}$		$\|a\|_{max}$	$\|a\|_{par}$	$\|a\|_{vol}$
Ordinary C64	49.00	470	47	0.289	48.24	554	76	0.423
10,000 ton C70	50.76	539	63	0.300	51.93	581	75	0.356
20,000 ton C80	46.12	558	66	0.192	44.78	745	70	0.219

From Table 5, it is observed that under the influence of the change in atmospheric temperature, the maximum, average, and effective acceleration during the frozen period are about 1.2 times larger than those during the non-frozen period. It is also found that the growth in ordinary C64 is the most significant. Further, the maximum accelerations during the freezing period and the non-frozen period also tend to increase as the axle load increases.

3.3.2. Frequency-Domain Analysis of Acceleration

FFT is conducted on the time-domain data of the vibration acceleration of C64, C70, and C80 to obtain the spectrum when the collection frequency is 1000 Hz and the frequency-domain analysis frequency is 0–500 Hz. The acceleration frequency spectrum curves are obtained while heavy haul trains pass by C1 during the frozen period and the non-frozen period, as shown in Figure 12.

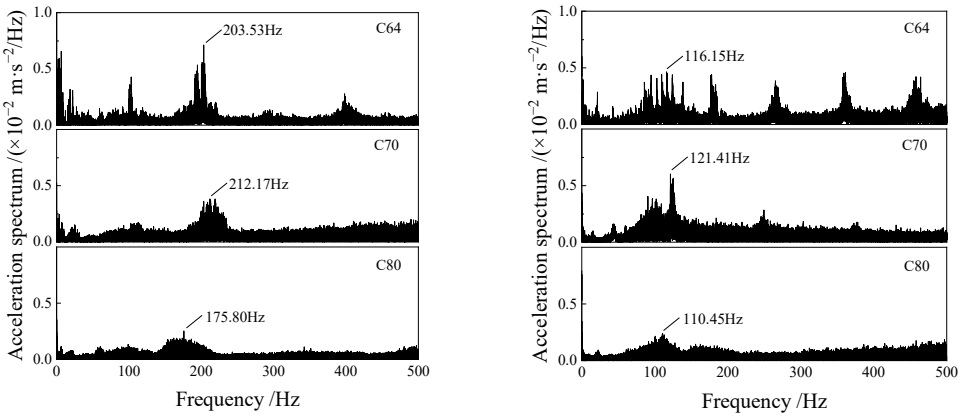

Figure 12. Spectra of vibration amplitude induced by a full-load train passing by C1: (**a**) non-frozen period; (**b**) freezing period.

From Figure 12, it can be observed that the main vibration frequency of the subgrade during the non-frozen period and the freezing period are 200 and 115 Hz, respectively. The main vibration frequency decreases while the vibration frequency range increases following the subgrade freezing. However, the lower-frequency vibration components are more abundant, indicating that the presence of the frozen soil layer prevents more high-frequency vibrations from propagating outward, resulting in a greater proportion of low-frequency components.

3.3.3. Attenuation Law of Vibration Response Acceleration of the Subgrade

The acceleration monitoring sites are located on the subgrade surface directly beneath the steel rail, and the acceleration demonstrated significant free attenuation after the train passed. The natural vibration frequency is determined by interpreting the residual vibration signals of the subgrade surface layer after the train passes. Figure 13 shows the vibration attenuation of C1 during the non-frozen period and the frozen period when the full-load C80 passed.

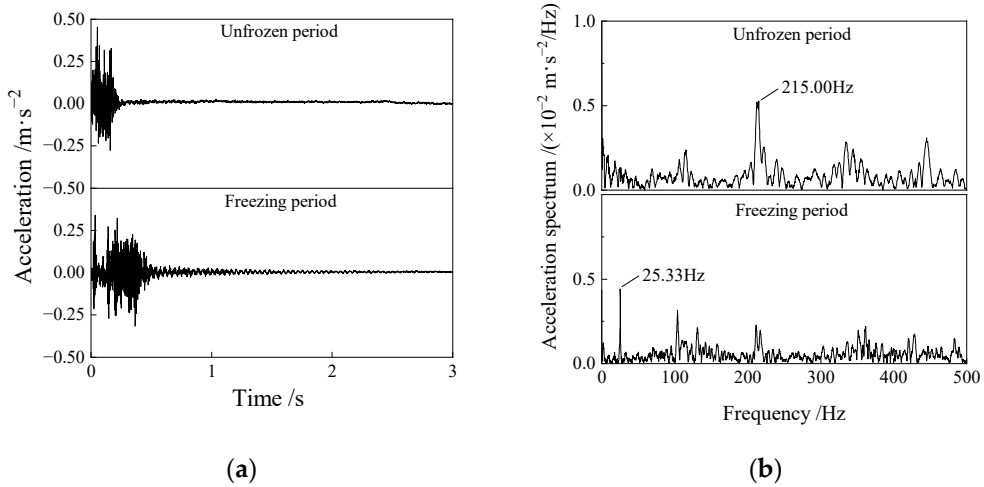

Figure 13. Attenuation of natural vibration acceleration of full-load C80 passing by C1: (**a**) vertical acceleration pickup signal; (**b**) vertical acceleration natural vibration signal power spectrum.

From Figure 13, it can be observed that an obvious natural vibration attenuation process is generated after the C80 train passes by the site, and it is also seen that the amplitude of acceleration decreases. Further, the main frequency of natural vibration caused due to the influence of the train after the subgrade freezing is found to be lower

than that before subgrade freezing. Table 6 lists the main frequencies of natural vibrations induced by the three heavy haul trains passing by C1 in a full-load status during the non-frozen and frozen periods.

Table 6. Vibration accelerations and main frequency of natural vibrations of different trains at C1 (Hz).

Train Type	Speed ($km \cdot h^{-1}$)	Main Frequency of Natural Vibration during the Non-Frozen Period (Hz)	Main Frequency of Natural Vibration during the Freezing Period (Hz)
Ordinary C64	48	23.6	117.4
10,000 ton C70	51	28.1	122.3
20,000 ton C80	45	26.2	122.3

As shown in Table 6, the subgrade has a larger rigidity after freezing, and the main frequency of natural vibration is significantly larger than that before freezing. Further, the non-frozen period vertical acceleration shows fast attenuation, and the freezing period has a significant impact on vertical acceleration. Moreover, the acceleration amplification effect due to frozen soil is evident [25]. This may be due to the migration of moisture in the lower part of the subgrade. They are constantly migrating upwards and are collected as ice near the freezing front [26]. This frozen part increases the strength and rigidity of the subgrade, thus resulting in an enlarged vertical acceleration amplitude. This is in good agreement with the results concluded from the time-domain analysis.

3.3.4. Response Features of Dynamic Speed and Dynamic Displacement before and after Freezing

The feasibility of employing the vibration response monitoring method to identify the subgrade frost heave disease is discussed to further analyze the impact of the subgrade frost heave on the subgrade vibration. In this paper, the dynamic speed and the dynamic displacement of the subgrade before and after freezing are summarized. Thereafter, the acceleration time–history data are filtered and then integrated to obtain the vibration speed time–history curve. Similarly, the time history of speed is filtered and integrated to obtain the dynamic displacement time–history curve [25].

(1) Dynamic speed before and after freezing.

Figure 14 shows the dynamic speed responses of full-load and no-load of C80 before and after freezing.

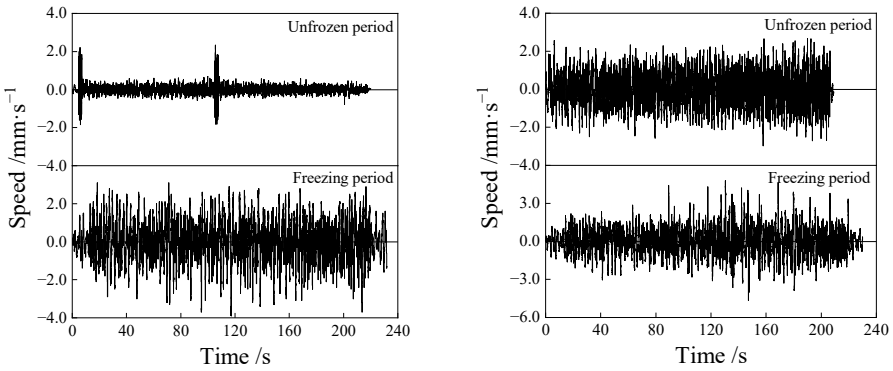

Figure 14. Time–history curves of vibration speeds of subgrade when (**a**) full-load C80 passing by C2 and (**b**) no-load C80 passing by C1.

As shown in Figure 14, the locomotive is responsible for the locomotive-induced maximum vibration speed before freezing, and the locomotive-induced vibration speed when the locomotive passes ranges from 1.51.5 to 2.2 mm/s. The vibration speed caused

by the coach is found to be less than 1.0 mm/s, and the vibration speed after freezing is significantly larger as the low-frequency noise component of the original acceleration signal is small. Moreover, the low-frequency part of the amplitude-spectrum of the acceleration signal significantly reduces, and there would be signal loss after filtering [27]. Furthermore, the vibration speed response does not present the same curve features as that of the acceleration. After freezing, the measured dynamic speed induced by a full-load train shows an increasing trend; however, the dynamic speeds of the locomotive and coach do not differ very much. The locomotive-induced vibration speed could not be reflected.

The calculation methods for calculating the maximum and average vibration speeds of different trains are similar to those for vertical vibration acceleration. Figure 15 shows the maximum and average vibration speeds of different trains. Herein, the values measured when full-load trains were passing by C1 and no-load trains were passing by C2 were employed.

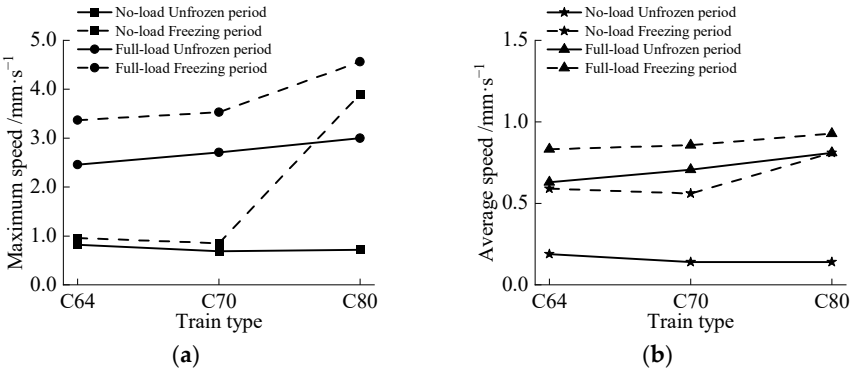

Figure 15. Dynamic speeds of different trains before and after freezing: (**a**) maximum vibration speed; (**b**) average vibration speed.

From Figure 15, it can be seen that the maximum and average vibration speeds after the freezing of the subgrade soil are both larger than those before freezing, where the maximum vibration speed induced by the full-load trains has a significant growth compared to those induced by no-load trains. The average vibration speed induced by no-load trains has a significant growth compared to those induced by full-load trains. Further, the maximum and average dynamic speeds induced by the full-load trains show an increasing trend as the axle load grows, while the maximum and average dynamic speeds induced by the no-load trains show a decreasing trend as the axle load declines.

(2) Dynamic displacement before and after freezing.

Figure 16 shows the dynamic displacement responses of the full-load and no-load C80 before and after freezing.

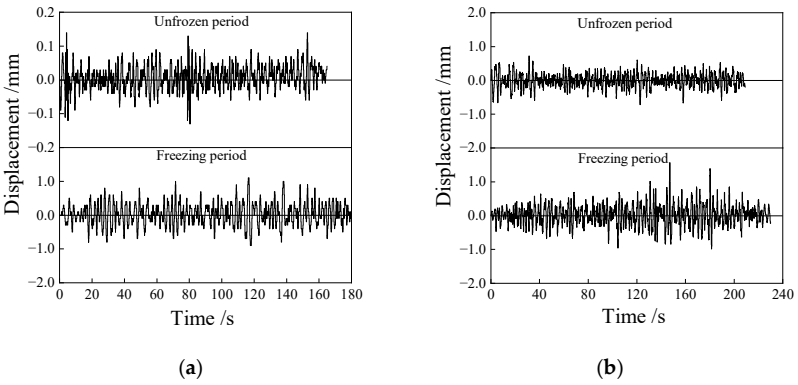

Figure 16. Time–history curves of dynamic displacements of (**a**) full-load C80 passing by C1 and (**b**) no-load C80 passing by C2.

The dynamic displacements induced by the locomotive during the non-frozen period significantly increase, as shown in Figure 16, while the dynamic displacements induced by the locomotive during the frozen period increase, which is not evident and only increases when the coach passes. Further, the maximum dynamic displacement induced by the no-load trains during the non-frozen period is almost 0.1 mm, while the maximum dynamic displacement induced by the no-load trains during the frozen period is 0.2~0.6 mm. This suggests that the dynamic displacement before freezing is 20% of the value observed after freezing. Moreover, the dynamic displacements induced by the full-load trains after freezing increase slightly, while dynamic displacements induced by no-load trains after freezing increase significantly when compared to those induced by full-load trains after freezing.

Figure 17 shows the maximum and average dynamic displacements induced by different trains. Herein, the values measured while the full-load trains passed by C1 and no-load trains passed by C2 were employed.

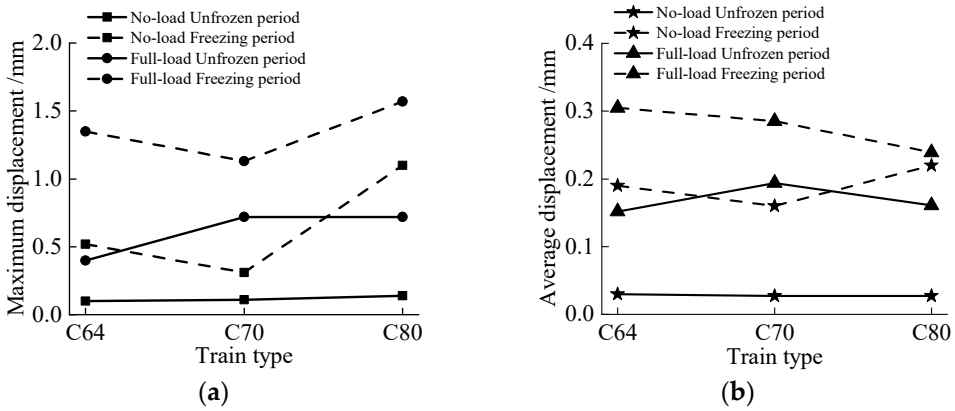

Figure 17. Dynamic displacements of different trains before and after freezing: (**a**) maximum dynamic displacement; (**b**) average dynamic displacement.

As shown in Figure 17, the dynamic displacements of different trains before and after freezing demonstrate a trend consistent with that of dynamic speed, and the values increase after freezing. The maximum dynamic displacement and the average vibration of the subgrade soil after freezing are larger than those before freezing. Furthermore, the maximum dynamic displacements induced by full-load trains increase significantly as compared to those induced by no-load trains, while the average dynamic displacements induced by the no-load trains increase significantly as compared to those induced by the full-load trains.

4. Discussions

The analysis of the subgrade dynamic response reveals that, except for the locomotive, train speed, and axle load directly affect the subgrade vibration acceleration amplitude. Moreover, the season is another major factor. Amplitude and frequency of vibration acceleration of the subgrade demonstrate significant variations after freezing, along with an enlarged vibration amplitude, reduced main vibration frequency caused by the train, and increased natural vibration frequency of soil. According to the monitored vertical acceleration, dynamic speed, and dynamic displacement before and after freezing, the maximum and average vertical acceleration, dynamic speed, and dynamic displacement exhibit growth after freezing in both full-load trains and no-load trains. As the subgrade froze from the subgrade surface downwards during the freezing period, the strength and stiffness of the subgrade increased. In the meantime, the uneven deformation along the subgrade is aggravated, thus causing an increase in vibration response, such as acceleration. This is in good agreement with the findings from other studies on the impact of seasonally frozen layers on the vibration responses of the subgrade [19–21]. However, another study [28]

concludes the opposite while investigating high-speed railway subgrade in seasonally frozen regions. In their work, the high-speed railway had strict requirements on ride comfort, and the difference in ride comfort between winter and summer was not significant. Moreover, during the freezing period, due to the existence of the frozen subgrade soil, the soil stiffness was improved. The overall stability of the subgrade is thus improved, which further leads to a decrease in the subgrade vertical vibration response, thus reducing the vibration response.

According to the vibration response characteristics of the subgrade before and after freezing, after frost heave generated by the subgrade freezing, the spectrum range of the acceleration vibration becomes larger, and the main vibration frequency becomes more pronounced as the spectrum distribution tends to move towards the lower frequency band. The existence of the frozen soil facilitates low-frequency and high-amplitude vibration. If a certain section of the subgrade is overly deformed due to severe frost heave, the interaction and vibration between line and train are aggravated when heavy haul trains pass during the freezing period. This affects the stability and safety of the train. Therefore, the vibration response monitoring method can be used to detect subgrade diseases in the section with frost heave, thereby improving the theory of frost heave. This provides a method to prevent and control freezing damage and also offers a reference for similar railway construction in the seasonally frozen region.

During the two monitoring periods considered in this paper, the ambient temperature does not drop to the average of the lowest temperature in previous years, and the freezing depth is shallow; thus, it has a certain impact on the dynamic response analysis. Further, the multiple freeze–thaw cycles should be monitored to understand the subgrade vibration response mechanism efficiently. The acceleration monitoring data can provide the basis for evaluating the stability and dynamic response of the subgrade under the action of trains and also provide theoretical support for experimental studies and numerical simulations in seasonally frozen regions.

5. Conclusions

From this work, the following conclusions can be drawn.

1. The train speed is a major factor affecting the maximum and average vibration acceleration, where the maximum vibration acceleration is commonly generated when the locomotive pass, and the vibration acceleration of coaches are usually smaller than that of the locomotive.
2. During the non-frozen period, when both full- and no-load heavy haul trains pass by, they possibly exert a certain impact on the surrounding environment of the dual lines. Moreover, the maximum and average acceleration measured when full-load heavy haul trains passed by C1 are much larger than those measured when no-load heavy haul trains passed by C2. Moreover, the maximum vertical acceleration induced by C80 is 1.534 m/s^2, which is lower than the limit value.
3. The maximum and average vertical acceleration, dynamic speed, and dynamic displacement are significantly increased after freezing. The frozen subgrade soil has an amplification effect on the vibration responses of the subgrade. The non-frozen period vertical acceleration, dynamic speed, and dynamic displacement are found to attenuate relatively fast, whereas the attenuation of the vertical acceleration, dynamic speed, and dynamic displacement during the frozen period is relatively slow. This implies that the frozen subgrade soil has an amplification effect on the vibration response and exerts a significant impact on the attenuation rate of the vibration response. Furthermore, the main frequency of the natural vibration is significantly higher than that before freezing.

Author Contributions: Conceptualization and methodology, Y.-Z.Z. and P.L.; funding acquisition, resources and supervision, Y.-Z.Z.; writing—original draft preparation, Y.-Z.Z. and Y.-Q.D.; validation

and data curation, Y.-Q.D. and X.-X.C.; investigation, P.L. All authors have read and agreed to the published version of the manuscript.

Funding: This research was funded by the National Natural Science Foundation of China (NSFC), grant numbers 52078312, 51978426, and 51708369, Science and Technology Development Foundation of Colleges and Universities in Hebei Province, grant number ZD2020335, Innovative Research Group Project of Natural Science Foundation of Hebei Province, grant number E2021210099 and Shijiazhuang Tiedao University Graduate Student Innovation Grant Program (YC2022019).

Institutional Review Board Statement: This study did not require ethical approval.

Informed Consent Statement: Not applicable.

Data Availability Statement: Not applicable.

Conflicts of Interest: The authors declare no conflict of interest.

References

1. Chen, Z.G. Research of the Reinforcing Design to the Subgrade Disease of Dazhun Railway. Master's Thesis, Southwest Jiaotong University, Chengdu, China, 29 April 2016. (In Chinese)
2. Zhang, Z.C.; Li, X.; Tian, Y.H.; Wei, C.X.; Zhang, G.G. Shear strength characteristics at different temperatures of Shenshuo Railway subgrade filling. *J. Chang. Univ.* **2017**, *37*, 60–66. (In Chinese) [CrossRef]
3. Zhai, W. *Vehicle-Track Coupled Dynamics: Theory and Application*; Springer Science Press: Beijing, China, 2020.
4. Song, Y.; Wang, Z.; Liu, Z.; Wang, R. A spatial coupling model to study dynamic performance of pantograph-catenary with vehicle-track excitation. *Mech. Syst. Signal Process.* **2021**, *151*, 107336. [CrossRef]
5. Galvín, P.; Domínguez, J. Experimental and numerical analyses of vibrations induced by high-speed trains on the Córdoba–Málaga line. *Soil Dyn. Earthq. Eng.* **2009**, *29*, 641–657. [CrossRef]
6. Qiu, M.M.; Yang, G.L.; Shen, Q.; Yang, X.; Wang, G.; Lin, Y.L. Dynamic behavior of new cutting subgrade structure of expensive soil under train loads coupling with service environment. *J. Cent. South Univ.* **2017**, *24*, 875–890. [CrossRef]
7. Gao, G.Y.; Yao, S.F.; Yang, J.; Chen, J. Investigating ground vibration induced by moving train loads on unsaturated ground using 2.5D FEM. *Soil Dyn. Earthq. Eng.* **2019**, *124*, 72–85. [CrossRef]
8. Omer, J.; Choi, D.H. Effect of track irregularities on the response of two-way railway tracks. *Appl. Sci.* **2020**, *10*, 11. [CrossRef]
9. Li, S.Y.; Lai, Y.M.; Zhang, S.J.; Yang, Y.G.; Yu, W.B. Dynamic responses of Qinghai-Tibet railway embankment subjected to train loading in different seasons. *Soil Dyn. Earthq. Eng.* **2012**, *32*, 1–14. [CrossRef]
10. Bahrekazemi, M. Train-Induced Ground Vibration and Its Prediction. Ph.D. Thesis, Royal Institute of Technology, Stockholm, Sweden, 13 February 2004.
11. Ren, X.W.; Wu, J.F.; Tang, Y.Q.; Yang, J.C. Propagation and attenuation characteristics of the vibration in soft soil foundations induced by high-speed trains. *Soil Dyn. Earthq. Eng.* **2019**, *117*, 374–383. [CrossRef]
12. Kaynia, A.M.; Madshus, C.; Zackrisson, P. Ground vibration from high-speed trains: Prediction and countermeasure. *J. Geotech. Geoenviron. Eng.* **2000**, *126*, 531–537. [CrossRef]
13. Connolly, D.P.; Kouroussis, G.; Woodward, P.K.; Costa, P.A.; Verlinden, O.; Forde, M.C. Field testing and analysis of high speed rail vibrations. *Soil Dyn. Earthq. Eng.* **2014**, *67*, 102–118. [CrossRef]
14. Petriaev, A. The vibration impact of heavy freight train on the roadbed. *Procedia Eng.* **2016**, *143*, 1136–1143. [CrossRef]
15. Kerr, A.D. *Track Mechanics and Track Engineering*; Track Department of Shanghai Institute of Railway Technology, Translator; Beijing China Railway Publishing House: Beijing, China, 1988; pp. 199–215. (In Chinese)
16. Li, S.Z.; Ling, X.Z.; Tian, S.; Ye, Y.S.; Tang, L.; Cai, D.G.; Wang, K. In-situ test and analysis of subgrade vibration with ballasted track in deep seasonally frozen regions. *Transp. Geotech.* **2021**, *31*, 100658. [CrossRef]
17. Zhu, Z.Y.; Ling, X.Z.; Wang, L.N.; Zhang, F.; Chen, S.J.; Wu, Q. Vibration characteristics of permafrost embankment induced by passing trains in Qinghai-Tibet railway in winter. In Proceedings of the 9th International Conference on Chinese Transportation Professionals, Harbin, China, 5–9 August 2009.
18. Chen, T.; Wu, Z.J.; Che, A.L.; Ma, W.; Shi, H. Test study on dynamic responses of railroad embankments in permafrost regions under train dynamic loading. *Earthq. Eng. Eng. Dyn.* **2011**, *31*, 168–173. (In Chinese) [CrossRef]
19. Ling, X.Z.; Zhang, F.; Zhu, Z.Y.; Ding, L.; Hu, Q.L. Field experiment of subgrade vibration induced by passing train in a seasonally frozen region of Daqing. *Earthq. Eng. Eng. Vib.* **2009**, *8*, 149–157. [CrossRef]
20. Ling, X.Z.; Wang, L.N.; Zhang, F.; Chen, S.J.; Zhu, Z.Y. Field experiment on train-induced embankment vibration responses in seasonally-frozen regions of Daqing, China. *J. Zhejiang Univ.-Sci. A* **2010**, *11*, 596–605. [CrossRef]
21. Dong, J.; Yang, Y.; Wu, Z.H. Propagation characteristics of vibrations induced by heavy-haul trains in a loess area of the North China Plains. *J. Vib. Control* **2019**, *25*, 882–894. [CrossRef]
22. Dong, J.; Wu, Z.H. Propagation laws of heavy -haul trains -induced ground vibration in seasonal frozen area of north China plain. *J. Vib. Shock.* **2018**, *37*, 286–291. (In Chinese) [CrossRef]

23. Zhu, Z.Y.; Ling, X.Z.; Zhang, F.; Hu, Q.L.; Chen, S.J. Field monitoring on vibration response of railway structure in the seasonally frozen region in summer. *J. Harbin Inst. Technol.* **2009**, *41*, 41–45. (In Chinese)
24. Gao, J.M.; Guo, Y.; Guo, Y. Dynamic influence of uneven frost heaving deformation of high-speed railway subgrade on wheel-rail system. *J. China Railw. Soc.* **2019**, *41*, 94–102. (In Chinese) [CrossRef]
25. Wang, Z.Y.; Ling, X.Z.; Zhu, Z.Y.; Zhang, F. Dominant frequencies of train-induced vibrations in a seasonally frozen region. *Cold Reg. Sci. Technol.* **2015**, *116*, 32–39. [CrossRef]
26. Zhang, Y.Z.; Yang, W.; Li, R.; Zhao, W.G.; Zhang, G.Y.; Li, P. Monitoring and rule analysis of frost heaving and thawing settlements of heavy haul railway roadbed in seasonal frozen region. *China Railw. Sci.* **2022**, *43*, 1–10. (In Chinese)
27. Zhou, Y.J. A Study on Integral Algorithm for Acceleration Test to Get Displacement and Application. Master's Thesis, Chongqing University, Chongqing, China, 1 May 2013. (In Chinese).
28. Tian, S.; Tang, L.; Ling, X.Z.; Ye, Y.S.; Li, S.Z.; Zhang, Y.J.; Wang, W. Field investigation into the vibration characteristics at the embankment of ballastless tracks induced by high-speed trains in frozen regions. *Soil Dyn. Earthq. Eng.* **2020**, *139*, 106387. [CrossRef]